Three-Dimensional Nonequilibrium Viscous Flow over the Shuttle Orbiter with Catalytic Surface Effects

M.D. Kim* and Clark H. Lewis†
Virginia Polytechnic Institute and State University, Blacksburg, Virginia

Computational results are presented for the three-dimensional nonequilibrium flowfield over the entire windward surface of a modified Shuttle-like geometry at high angles of attack (up to 50 deg). The viscous shock-layer method used takes into account the finite rate chemical reactions of multicomponent ionizing air, and the governing equations are written in a general nonorthogonal computational grid system. Boundary conditions considered include noncatalytic wall, finite catalytic wall, fully catalytic wall, and nonequilibrium slip conditions at the wall and/or shock. The nonequilibrium solutions are compared with equilibrium air solutions, perfect gas solutions, and Shuttle flight heat-transfer and pressure data, and the comparisons show good agreement and correlations between the nonequilibrium solutions and the flight data. Three-dimensional effects are clearly shown in the flight derived data for the first time based upon the results of this study.

Nomenclature

C_i = concentration of species i, ρ_i/ρ
C_p = specific heat at constant pressure
FINCAT = nonequilibrium solution with finite catalytic wall
FULCAT = nonequilibrium solution with fully catalytic wall
k_w = surface catalytic recombination rate
k_{wi} = surface catalytic recombination rate of species i
L = Shuttle body total length, 32.84 m
Le = Lewis number
M_i = species molecular weight
M_∞ = freestream Mach number
NONCAT = nonequilibrium solution with noncatalytic wall
NONEQL = nonequilibrium flowfield solution
NSH/RN = shock-layer thickness nondimensionalized by R_n
p = pressure, $p^*/\rho_\infty U_\infty^2$
PG = perfect gas solution
PHI = same as ϕ in cylindrical coordinates
Pr = Prandtl number
PW/PINF = nondimensional wall pressure, p_w^*/p_∞
QW = heating rate due to conduction and diffusion, MW/m^2
R = universal gas constant
Re_∞ = freestream unit Reynolds number, m^{-1}
R_n = dimensional Shuttle nose radius, 62.23 cm (24.5 in.)
s = surface distance along body
SHTNEQ = Shuttle nonequilibrium, the present numerical method
STS = space transportation system
S/RN = nondimensional surface distance along body, s^*/R_n
T = temperature, T^*/T_{ref}
T_{ref} = dimensional reference temperature, $U^2_\infty/C_{p\infty}$
t = Shuttle entry time from 122 km altitude interface
u,v,w = streamwise, normal, and circumferential velocity components nondimensional by U_∞
U_∞ = dimensional freestream velocity
U/UINF = streamwise velocity, u^*/U_∞
$\dot{w}_i$ = species production term
Y/RN = distance in body-normal direction, ξ_2/R_n
z,r,ϕ = reference cylindrical coordinates
Z/L = nondimensional axial distance along body, z^*/L
α = angle of attack, deg
γ_i = species catalytic recombination coefficient
ϵ = Reynolds number parameter, $\epsilon^2 = \mu_{\text{ref}}/(\rho_\infty U_\infty R_n)$
η = body-normal coordinate normalized by shock-layer thickness
μ = viscosity, μ^*/μ_{ref}
μ_{ref} = reference viscosity evaluated at T_{ref}
ξ_1,ξ_2,ξ_3 = body-generator computational coordinates
ρ = density, $\rho^*\rho_\infty$

Superscript

( )* = dimensional quantity

Subscripts

i = species i
ref = dimensional reference quantity
w = wall value
∞ = dimensional freestream value

Introduction

RECENTLY the nonequilibrium effects on the shuttle re-entry flowfield have been widely investigated to better understand the sensitivity of the surface heating to catalytic recombination caused by the heatshield material. Various numerical methods have been applied to solve the nonequilibrium viscous flowfield over the windward surface of the Space Shuttle during re-entry. For instance, Miner and Lewis[1] developed a two-dimensional nonequilibrium viscous shock-layer method and applied it to solve the flowfield in the windward symmetry plane of the Space Shuttle using an "equivalent axisymmetric body" concept. Shinn et al.[2] analyzed the effects of a finite catalytic wall on the heating rate along the Shuttle windward symmetry plane using a two-dimensional nonequilibrium viscous shock-layer method. They also used the equivalent axisymmetric body concept. Rakich and Lanfranco,[3] Rakich et al,[4] and Scott and Derry[5]

Presented as Paper 83-1426 at the AIAA 18th Thermophysics Conference, Montreal, Canada, June 1-3, 1983; received June 20, 1983; revision received Jan. 10, 1984.

*Graduate Student, Aerospace and Ocean Engineering Department. Student Member AIAA.

†Professor, Aerospace and Ocean Engineering Department. Associate Fellow AIAA.

calculated the Shuttle windward centerline heating distribution by combining three-dimensional inviscid flow solutions with reacting two-dimensional axisymmetric analog boundary-layer calculations, including the finite catalytic wall effect.

However, none of the foregoing methods could solve the three-dimensional reacting viscous flowfield at high angle of attack without a major approximation such as the axisymmetric analog or the equivalent axisymmetric body concept. The purpose of the present work is to describe a method to predict the three-dimensional nonequilibrium flowfield over the entire windward surface of the Space Shuttle Orbiter using the recently developed SHTNEQ code by Kim et al.[6] The computational results obtained are compared with the flight heating rate and pressure data. The present three-dimensional viscous shock-layer method (SHTNEQ) takes into account the finite rate chemical reactions of multicomponent ionizing air. A general nonorthogonal computational grid system was introduced to treat the nonaxisymmetric Shuttle geometry. The present method can solve both subsonic and supersonic flows and requires the shock shape as initial input data.

It is known that the nonequilibrium real gas effects persist over a wide range of the Shuttle re-entry trajectory (altitudes of 122-50 km). In the present work, three points along the trajectory of the second Space Shuttle flight (STS-2) are chosen, and the numerical solutions are obtained over the entire windward surface of the body. The altitudes chosen are 85.74, 74.98, and 71.29 km designated as cases 1, 2 and 3, respectively. The nose radius used as the reference length is 0.62318 m. The Reynolds number parameter ϵ is 0.10766 for case 1, 0.04394 for case 2, and 0.03286 for case 3. For each test case numerical predictions have been obtained for the following chemical models: 1) nonequilibrium air with finite catalytic wall, 2) nonequilibrium air with noncatalytic wall, 3) nonequilibrium air with fully catalytic wall, 4) equilibrium air, and 5) perfect gas. All of the predictions are compared with the flight measurement data. The present numerical scheme was extended further to include the capability to treat the nonequilibrium wall- and shock-slip conditions. In order to demonstrate the "three-dimensional effects" on the surface heating rate, as well as the other surface-measureable quantities, the present SHTNEQ method has also been applied to the "equivalent axisymmetric body" of the Space Shuttle Orbiter at high angles of attack.

Analysis

For a general three-dimensional vehicle such as the Shuttle Orbiter, a proper geometry definition is a prerequisite for an accurate flowfield analysis. Using the QUICK method developed by Vachris and Yaeger,[7] the geometry of the Orbiter was represented by a series of analytical functions in a cylindrical coordinate system (z,r,ϕ). The primary region of interest was the windward surface of the Shuttle. A modified Shuttle-like geometry which has the same lower surface and upper-symmetry plane profile is shown in Fig. 1. For the modified geometry, the region between the strake and wing leading edge and the upper symmetry plane was filled in with elliptic curves. Nevertheless, the windward side geometry is a good representation of the Space Shuttle up to about $\phi = 80$ deg. A surface-oriented nonorthogonal coordinate system was used in the present analysis. The ξ_1 coordinate starts from the body nose tip and is directed along the body on the body surface. The ξ_3 coordinate starts from the windward symmetry plane and is directed around the body. At the body surface the ξ_3 coordinate is chosen to coincide with the ϕ coordinate of the reference cylindrical coordinate system. The ξ_2 coordinate is a straight line from the body surface to the shock surface. The ξ_2 coordinate lines are always normal to the local body surface. In the present analysis the ξ_2 coordinate is normalized by the local shock stand-off distance. A detailed description of the procedure for coordinate and grid generations for a similar coordinate system is given in Ref. 8.

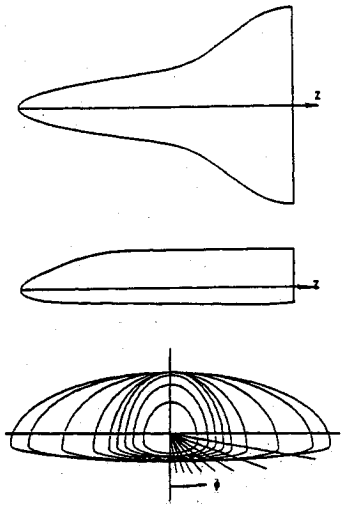

Fig. 1 Cross sections of the modified Shuttle Orbiter.

Governing Equations

The governing equations are derived from the steady Navier-Stokes equations for a reacting gas mixture as given by Bird et al.,[9] written in a surface-oriented general nonorthogonal coordinate system. The present analysis follows the formulations of two-dimensional reacting flow by Miner and Lewis[1] and three-dimensional perfect gas flow by Szema and Lewis.[10] The normal velocity v and normal coordinate ξ_2 are assumed to be on the order of ϵ, and all terms which are of higher order are neglected in the governing equations to obtain a single set of equations. The equations are parabolic in both streamwise and transverse directions. Only laminar flow is considered in the present analysis. Detailed governing equations are given in Ref. 6.

Boundary Conditions

At high-altitude (50-120 km), low Reynolds number flight, the Knudsen number is finite and the continuum model of the gas breaks down in the Knudsen layer where large gradients of the properties exist. At the body surface, the velocity-slip and temperature-jump boundary conditions can be used. In the present analysis, these nonequilibrium wall-slip equations for a spherical geometry, given by Hendricks,[11] have been rewritten for the present body-oriented general coordinate system and chemical model. The wall temperature is specified by the STS-2 flight thermocouple data. In the present calculations, the wall species concentrations are dictated by noncatalytic, fully catalytic, or finite catalytic conditions. For hypersonic nonequilibrium air flow, the surface heating rate is strongly affected by surface catalytic activity to the recombination of the dissociated oxygen and nitrogen atoms. For a nonequilibrium flow over a finite catalytic wall, the wall species concentration is dictated by the catalytic recombination rate k_w^* in the following expression:

$$\partial C_i/\partial\eta - (k_{wi}\rho Pr/Le/\mu/\epsilon^2)\,C_i = 0 \tag{1}$$

where $k_{wi}^* = k_{wi}^*/U_\infty$ is a nondimensional recombination rate. The catalytic recombination coefficient γ_i is related to k_w^* by

$$\gamma_i = \sqrt{2\pi M_i^*/R^*}/T^* k_{wi}^* \tag{2}$$

The recommended curve-fit expressions by Scott and Derry[5] are

$$\gamma_N = 0.071\exp(-2219/T_w) \text{ for } 1670\,\text{K} > T_w > 950\,\text{K} \tag{3}$$

$$\gamma_O = 16.0\exp(-10271/T_w) \text{ for } 1650\,\text{K} > T_w > 1400\,\text{K} \tag{4}$$

The above two equations may be rewritten for k_w^* (cm/s) as

$$k_{wN}^* = 69.484\sqrt{T_w}\exp(-2219/T_w) \quad (5)$$

$$k_{wO}^* = 14564\sqrt{T_w}\exp(-10271/T_w) \quad (6)$$

The curve-fit relations for oxygen given by Rakich et al.[4] are

$$k_{wo}^* = 66000\exp(-8017)/(T_w) \text{ for } 2000\text{ K} > T_w > 862\text{ K} \quad (7)$$

$$k_{wo}^* = 53\exp(-1875/T_w) \text{ for } 862\text{ K} > T_w > 500\text{ K} \quad (8)$$

At the low surface temperature of the Shuttle, the equilibrium catalytic wall condition can be replaced by the fully catalytic wall condition.

At low-density flight conditions the bow shock may have a finite thickness. In that case, after-shock quantities must be obtained by Davis.[12] In the present analysis, the numerical iteration scheme of the three-dimensional shock/boundary conditions with slip for perfect gas by Murray and Lewis[13] have been extended to include the finite rate chemistry and the nonorthogonal coordinate system. The complete set of the modified Rankine-Hugoniot shock-crossing relations written in the shock-normal coordinate for reacting gas flows is given in Ref. 6.

Thermodynamic and Transport Properties

The specific heat C_p and static enthalpy h are required for each of the species considered and for the gas mixture. Also required are the viscosity μ and the thermal conductivity k. Since the multicomponent ionizing air is considered to be a mixture of thermally perfect gases, the thermodynamic and transport properties for each species are calculated using the local temperature. The properties for the gas mixture are then determined in terms of the individual species properties. Since the present analysis follows the formulation of Miner and Lewis,[1] except for the mixture viscosity and conductivity, more details can be found in Ref. 1.

The viscosity and thermal conductivity of the gas mixture are calculated by the method suggested by Armaly and Sutton.[14,15] It in known that Armaly's method gives more accurate predictions than the well-known Wilke's semiempirical relations, especially at high temperatures. In the present work, the diffusion model is limited to binary diffusion with the binary diffusion coefficient specified by the Lewis number of 1.4.

Chemical Reaction Model

It is assumed that the chemical reactions proceed at a finite rate, and the rate of production terms $\dot{w}_i$ of the individual species are included in the energy equation and the species continuity equations. The $\dot{w}_i$ terms are functions of both the temperature and the species concentrations, and they must be rewritten so the temperature or the species concentrations appear as one of the unknowns as given in Ref. 1.

In the present calculations the chemical reaction model and the reaction-rate constants are taken from Blottner et al.[16] The seven reaction equations for seven species (O, O_2, NO, N, NO^+, N_2, e^-) are given as:

$$O_2 + M_1 = 2O + M_1$$

$$N_2 + M_2 = 2N + M_2$$

$$N_2 + N = 2N + N$$

$$NO + M_3 = N + O + M_3$$

$$NO + O = O_2 + N$$

$$N_2 + O = NO + N$$

$$N + O = NO^+ + e^- \quad (9)$$

The chemical production terms are calculated from the rate constants and species mass fractions, and detailed relations are given in Ref. 1. Since the rate of production terms is for nonequilibrium flows, the present method encounters difficulty in obtaining a converged solution whenever the flow conditions are very near chemical equilibrium. The difficulty is severe, particularly at the stagnation point.

Numerical Solution

Davis[17] presented an implicit finite-difference method to solve the viscous shock-layer equations for axially symmetric flows, and Murray and Lewis[13] developed the scheme further for three-dimensional flows. In the present work, the method is extended to the chemically reacting three-dimensional flowfield solution in a surface-oriented nonorthogonal coordinate system. Since the viscous shock-layer equations are parabolic in both the streamwise and cross-flow directions, the equations are solved by a highly efficient finite difference scheme. The continuity and normal momentum equations are solved in a coupled form to promote convergence. The shock standoff distance is evaluated by integrating the continuity equation.

The solution begins on the spherically blunted nose by obtaining an axisymmetric solution in the wind-fixed coordinate system. The axisymmetric solution is rotated into the body-fixed coordinates and is used as the initial profile for the three-dimensional solution. The three-dimensional solution begins in the windward plane and marches around the body obtaining a converged solution at each ξ_3 step. After completing a sweep at a ξ_1 marching station, the procedure then steps downstream in ξ_1 and begins the next ξ_3 sweep.

A solution may fail to converge when a geometry is complex and/or the angle of attack is extremely high. In order to overcome the convergence problem, a more refined shock input may be used. Applying a larger damping factor during a local iteration may also promote convergence. In the present analysis, the explicit pressure gradient model has been used over the rear half of the body to promote convergence.

Results and Discussion

In order to predict the Shuttle re-entry flowfield three test cases were chosen, and the viscous windward flowfield solutions were obtained using various chemical models. The altitudes selected for the present calculations are 81, 70, and 60 km, and the detailed freestream conditions for the three test cases are given in Table 1.

The inviscid input shock shapes for the present calculations have been provided by the HALIS method[18] for an angle of attack of 40 deg for both perfect gas and equilibrium air, but the inviscid HALIS shock was available only up to $z/L = 0.5$. The viscous flowfield solutions for both perfect gas and equilibrium air have been obtained up to $z/L = 0.5$ in order to compare them with the nonequilibrium solutions. The nonequilibrium solutions, however, were obtained for the entire windward surface up to the body end using an extrapolated shock. The shock extension was performed using the STEIN[19] solution of the shock shape for an angle of attack of 25 deg. The extrapolated shock was scaled and smoothed before being used as input data. In order to enhance the accuracy of the nonequilibrium viscous solution, a global iteration was performed using the viscous output shock as an input.

For hypersonic nonequilibrium flow, the surface heating rate is strongly affected by surface catalytic activity to the recombination of the dissociated oxygen and nitrogen atoms. Previously, most investigators tended to assume fully catalytic or equilibrium catalytic walls in order to obtain a more conservative solution of the heating rate. Recently, however, Rakich et al.[4] determined that the Shuttle reaction cured glass (RCG) coating is almost noncatalytic through their analysis of experimental flight data. However, depending on altitude condition, the present computational

Table 1 Test case freestream conditions

Case no.	t, s	Attitude, km	α, deg	M_∞	Re_∞, m^{-1}	U_∞, km/s	T_∞ K	p_∞, atm
1	250	85.74	41.0	26.6	2,726	7.53	199	3.587 $E-06$
2	460	74.98	40.0	25.5	15,686	7.20	198	2.142$E-05$
3	650	71.29	39.4	23.4	25,756	6.73	205	3.965 $E-05$

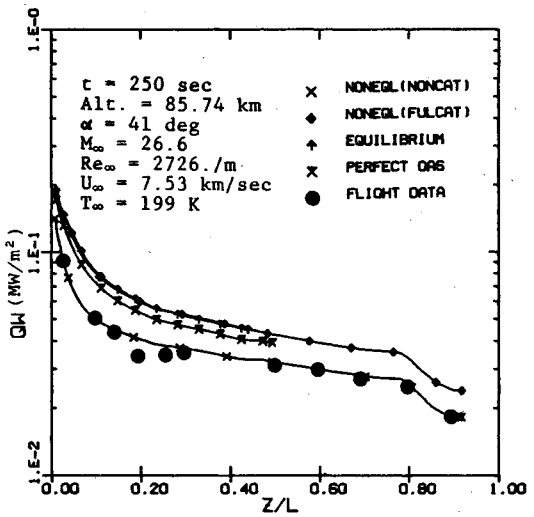

Fig. 2 Comparison of measured and calculated heating rates along the windward centerline of case 1.

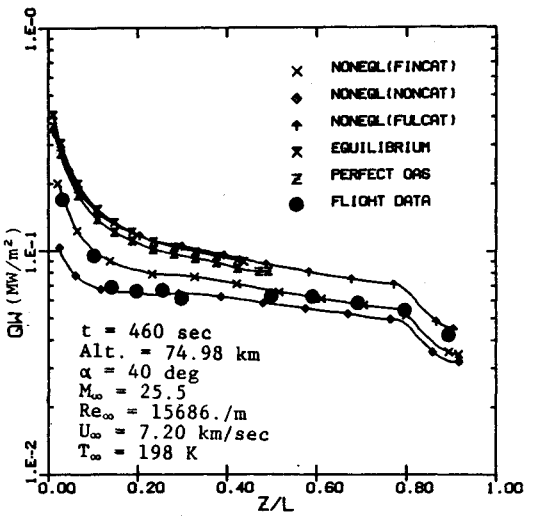

Fig. 3 Comparison of measured and calculated heating rates along the windward centerline of case 2.

analysis shows that the catalytic effect on the heating rate is not negligible, especially in the nose region.

Surface Heating Rate

The heating rate predictions along the windward centerline are presented in Fig. 2 for case 1. The nonequilibrium solution with a noncatalytic wall condition agrees well with the flight data for most of the region. The agreement is excellent considering the uncertainty of 10% in the flight data[4] and also the uncertainty of the gas-phase reaction rates. The nonequilibrium solution with a fully catalytic wall condition shows relatively close agreement with the equilibrium air solution. The heating rate prediction from the perfect gas model is below the equilibrium air solution but well above the noncatalytic wall solution for the entire body. The reason for the local mismatch with flight data around $z/L=0.2$ is not currently known. At $z/L=0.4$, the perfect gas solution is 20% lower than the equilibrium solution and 50% higher than the noncatalytic wall solution. For case 1 the finite catalytic wall solution using Scott's data was quite close to the noncatalytic wall solution (within 4%). The decrease of the heating after $z/L=0.8$ is due to the slope change of the body surface.

For cases 2 and 3, the general trends of the computed heating rates are similar to the results of case 1, but the noncatalytic wall solution underpredicts the flight data, especially in the nose region, as shown in Figs. 3 and 4. The result from the finite catalytic wall condition using Scott's relation agrees well with the flight data over most of the region. However, the reason for the local mismatch around $z/L=0.2$ for case 2 is not clearly understood. Surface heating rate has also been computed using Rakich's catalytic rate data[4] for case 2, and the result obtained was almost the same as the resultr from Scott's data.[5] For case 3, the finite catalytic wall solution overpredicts the flight data by about 10% on the forward half of the body, and agrees well over the rear half of the body. The mismatch may be partially due to the uncertainty of the surface catalytic recombination rate data. In Ref. 5, Scott discussed the possibility of overprediction in the arc-jet catalysis measurements due to contamination of the jet flow. The average uncertainty of

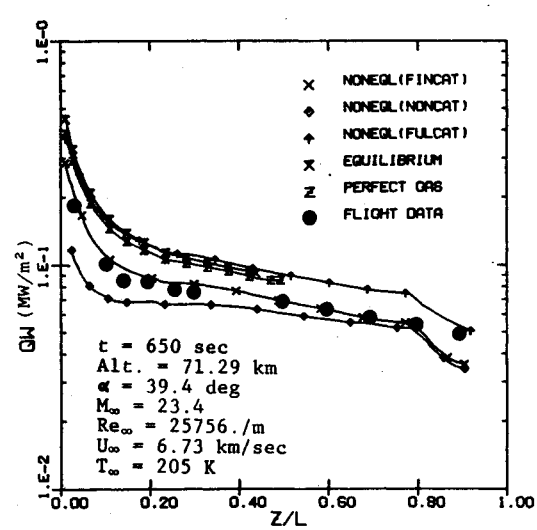

Fig. 4 Comparison of measured and calculated heating rates along the windward centerline of case 3.

Scott's measurement of surface catalysis was about 10% although there were many fluctuations in the uncertainties at each data point. The calculated spanwise heating rates from case 2 at $z/L=0.2$ are shown in Fig. 5. The comparisons among the various chemical models show similar trends and correlations for the spanwise heating rate distributions.

Surfaced Pressure and Shock-Layer Thickness

The surface pressure distributions over the entire Shuttle windward surface are presented in Fig. 6 together with the available flight data for comparison. The ϕ planes from 10 to 40 deg were omitted on the plots because the results for those planes were almost identical with the result for the windward centerline. The agreement with flight data is good, especially on the windward centerline. In Fig. 7 the spanwise surface pressure distributions are shown at $z/L=0.1$. The present calculation tends to underpredict in the flow expansion region

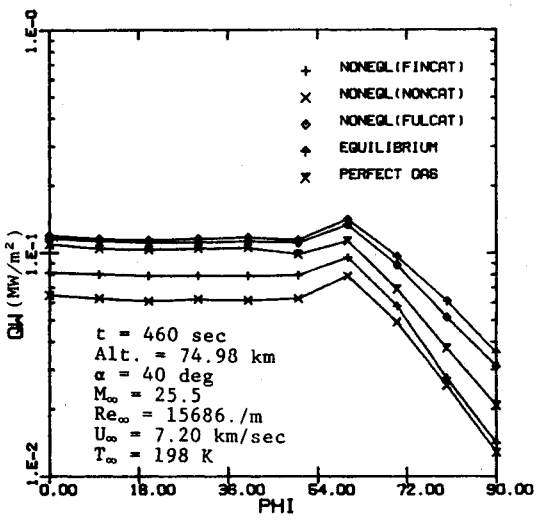

Fig. 5 Comparison of spanwise heating rate distributions at $z/L = 0.2$ for case 2.

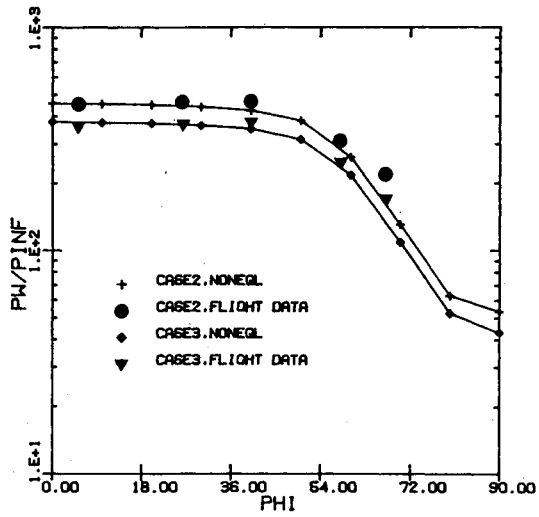

Fig. 7 Comparison of surface pressure distribution around the body with flight data at $z/L = 0.1$.

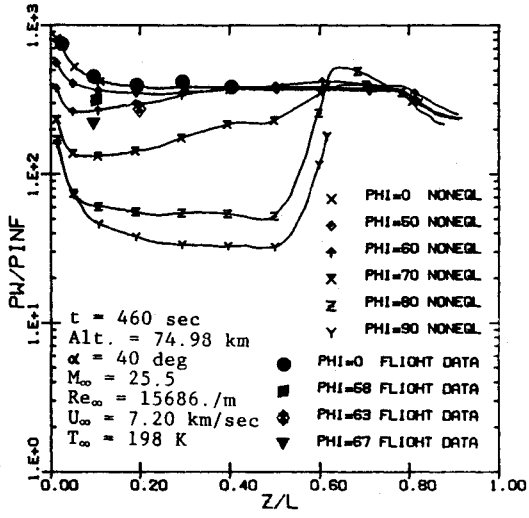

Fig. 6 Comparison of surface pressure distribution along the body with flight data for case 2.

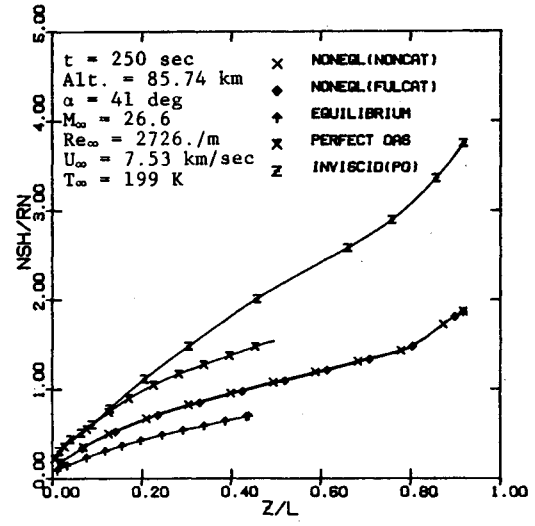

Fig. 8 Comparison of globally iterated solutions of windward shock-layer thickness distributions for case 1.

(off the centerline) compared to the flight data (e.g., about 20% underprediction at $\phi = $ deg, $z/L = 0.1$). The disagreement may be due partly to the uncertainty in the flight data, or a calculation using a smaller ϕ step size may reduce the discrepancy. The present solution by the SHTNEQ method used a ϕ step size of 10 deg around the body, and this step size may not be small enough for the noncircular cross sections of the Shuttle geometry (see Fig. 1). By including more ϕ planes, however, the current relatively large storage requirement and computing time must be increased accordingly.

A comparison is shown in Fig. 8 of the shock-layer thickness distributions along the body at the $\phi = 0$ plane which have been obtained from various chemical models. All of the viscous shock data are from the once globally iterate results. When the various viscous shock-layer thicknesses are compared to the inviscid perfect gas shock at $z/L = 0.4$, the viscous perfect gas shock is 86.7%, the nonequilibrium shock is 52.8%, and the equilibrium shock is 36.1%. The shock from the fully catalytic wall condition is almost identical to the noncatalytic wall solution.

Slip Effects

The SHTNEQ method has been extended further to included the shock- and wall-slip conditions. In high-altitude freestream conditions, the conventional frozen shock crossing of Rankine-Hugoniot relations for nonequilibrium flows gives a poor prediction of the after-shock quantities. It is known that the slip effects on surface-measurable quantities such as heating rate and pressure distributions are significant, especially for re-entry bodies with a small nose radius at high altitude (50-120 km). For the Space Shuttle at the test case freestream conditions, however, the calculated Reynolds number parameter ϵ was less than 0.108, which indicates that the slip effects on the surface-measurable quantities will not be significant.[17] But, the slip effects on some shock-layer profiles are not negligible, and, hence, are calculated and presented over the nose region.

In Fig. 9, the shock-slip effects on the temperature profile and mass fraction of oxygen and nitrogen atoms are shown at the stagnation point. The slip temperature at the shock is less than the no-slip temperature by 1500 K. The shock-slip effect on the oxygen mass-fraction distribution across the shock layer is limited to the region near the bow shock, but for nitrogen the shock-slip effect is propagated throughout the shock layer. Figure 10 shows the wall-slip effects on the surface temperature and axial flow velocity jump over the nose region for case 2. The amount of temperature jump is about 200 K at the stagnation point, and the slip velocity is 0.0056 times the freestream velocity at $s/R_n = 0.8$.

Comparison with Equivalent Axisymmetric Body

In order to demonstrate the "three-dimensional effects," the present method was also applied to the equivalent axisymmetric body, and the results are compared to the

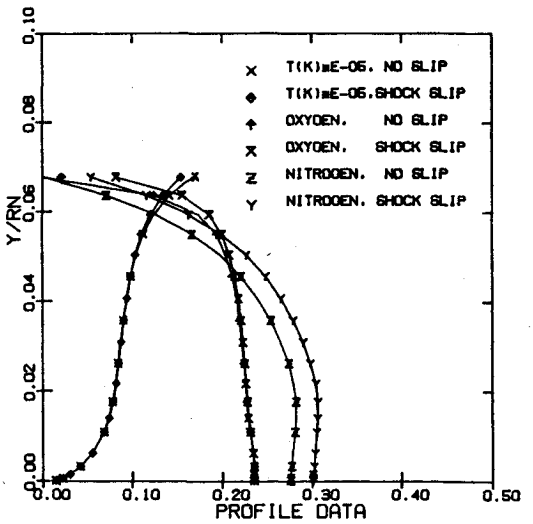

Fig. 9 Shock-slip effects on the profiles of temperature and mass fraction at the stagnation point for case 2.

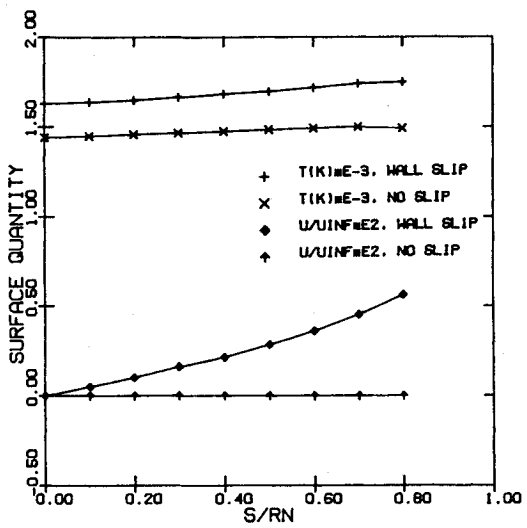

Fig. 10 Wall-slip effects on velocity slip and temperature jump in the nose region of case 2.

solution for the actual Shuttle geometry. The equivalent axisymmetric body is obtained by taking the windward centerline on the Shuttle surface and making a body of revolution around the wind axis passing through the physical stagnation point of the Shuttle at high angle of attack. The resulting body has a shape similar to a sphere cone of about 45 deg half-cone angle. Shinn et al.[2] replaced the actual Shuttle windward centerline with an equivalent hyperboloid in order to apply the two-dimensional reacting viscous shock-layer method.

In the present analysis, the equivalent axisymmetric body is generated using the actual Shuttle windward centerline defined by the QUICK geometry package, since the present SHTNEQ method can treat nonanalytic geometries. At high angle of attack (about 40 deg in the test cases), the equivalent axisymmetric body has a very large cross-sectional diameter, especially in the afterbody region, which may produce a solution different from the accurate three-dimensional solution for the original Shuttle geometry.

The present SHTNEQ method was applied to both the actual Shuttle geometry and the equivalent axisymmetric body, and the results are compared with each other. Figure 11 shows the comparison of the surface heating rates. The result from the two-dimensional viscous shock-layer by Shinn et al.[2] is also included for comparison. Both solutions from the

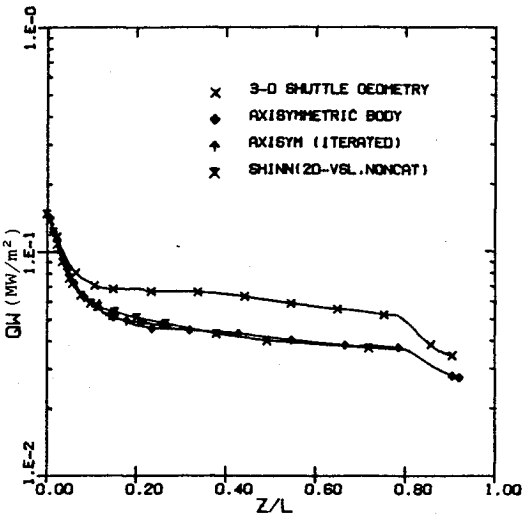

Fig. 11 Heating rate comparison with the equivalent axisymemtric body concept for case 3.

axisymmetric body concept underpredict by about 30% compared to the present three-dimensional Shuttle solution. Therefore, the equivalent axisymmetric body should not be used to simulate the actual three-dimensional Shuttle geometry at high angles of attack. The result from the second global iteration is also presented for the forward part of the axisymmetric body, which indicates that the result from the first global iteration is already a well converged solution. The skin friction for the three-dimensional body was 50% higher than the one for the axisymmetric body. Surface pressure distriubtion along the body for three-dimensional body was about 5-10% lower than the axisymmetric body solution. The shock-layer thickness from the axisymmetric body concept was much thicker than the one from the three-dimensional Shuttle geometry (about 1.5 times at the body end). Thus, the present analysis shows that the actual Shuttle geometry must be used in the three-dimensional numerical simulation in order to obtain an accurate prediction of the Shuttle nonequilibrium flowfield, especially in the case of high angle of attack.

Computing Times

The computing times required for the flowfield computations of all the test cases are listed in Table 2. The computing times are based on an IBM 370/3081 general-purpose computer. The nonequilibrium computation took about 1½ h of CPU time to solve the entire Shuttle windward surface. The computing times for the perfect gas and equilibrium air are for the solution of the first half of the body (up to $z/L=0.5$). The solution of the perfect gas or equilibrium air flows took relatively small computing times (less than 20% of the nonequilibrium case).

The axial marching step sizes are controlled internally in the code considering the number of local iterations taken. A fixed input of 51 or 101 grid points was used in the surface-normal direction and 10 planes were around the body for the windward surface (10-deg step-size). The leeward surface of the Space Shuttle was not considered because a solution cannot be obtained by the present method due to cross-flow separation. The storage requirement of the present SHTNEQ code is 852 kbytes in an IBM 370/3081 computer.

Conclusions

In general, the computational results of surface heating rate for the three-dimensional nonequilibrium flowfield over the Space Shuttle compare well with the available flight data. The flight heating rate data agree well with the noncatalytic wall solution for case 1 and are lower than or agree well with the

Table 2 Computing times[a] for test cases

Flow model	Case no.	z/L	Grid points in ξ_1	ξ_2	ξ_3	CPU time, h:min:s
NONEQL (finite catalytic)	1	0-0.93	127	51	10	1:22:47
	2	0-0.93	129	51	10	1:40:32
	3	0-0.93	142	51	10	1:43:03
NONEQL (non-catalytic	1	0-0.93	127	51	10	1:20:34
	2	0-0.93	129	51	10	1:50:28
	3	0-0.93	142	51	10	1:51:50
NONEQL (fully catalytic)	1	0-0.93	123	51	10	1:23:02
	2	0-0.93	124	51	10	1:26:53
	3	0-0.93	124	51	10	1:27:22
Perfect gas	1	0-0.50	78	101	10	0:07:07
	2	0-0.50	78	101	10	0:07:06
	3	0-0.50	78	101	10	0:07:05
Equilibrium	1	0-0.453	72	101	10	0:08:32
	2	0-0.453	72	101	10	0:08:28
	3	0-0.453	72	101	10	0:08:27

[a]CPU time on IBM 370/3081, H = OPT2 compiler.

finite catalytic wall solution for cases 2 and 3. The nonequilibrium solution with fully catalytic wall gives close agreement with the chemical equilibrium heating rate prediction and substantially overpredicts the flight data.

The calculated pressure distributions also show good agreement with the flight data. The calculated nonequilibrium shock- and wall-slip effects on the heating rate and surface pressure were negligible for the present test cases. The present parametric study of the surface catalytic effect shows that a proper chemical model and accurate catalytic recombination rate data are very important for an accurate prediction of the Shuttle surface heat transfer.

From the numerical analysis using the equivalent axisymmetric geometry, it is demonstrated that the three-dimensional effect on the surface-measurable quantities is not negligible in the case of high angle of attack, and, hence, a three-dimensional solver such as SHTNEQ should be used for an accurate nonequilibrium flowfield prediction. The computing times taken for the nonequilibrium calculation are reasonable, considering the large size of the computational grid due to the complex Shuttle geometry and the finite chemical reaction rates of the seven species.

References

[1]Miner, E.W. and Lewis, C.H., "Hypersonic Ionizing Air Viscous Shock-Layer Flows over Nonanalytic Blunt Bodies," NASA CR-2550, May 1975.

[2]Shinn, J.L., Moss, J.N., and Simmonds, A.L., "Viscous Shock-Layer Heating Analysis for the Shuttle Windward Plane with Surface Finite Catalytic Recombination Rates," AIAA Paper 82-0842, June 1982.

[3]Rakich, J.V. and Lanfranco, M.J., "Numerical Computation of Space Shuttle Laminar Heating and Surface Streamlines," *Journal of Spacecraft and Rockets,* Vol. 14, May 1977, pp. 265-272.

[4]Rakich, J.V., Stewart, D.A., and Lanfranco, M.J., "Results of a Flight Experiment on the Catalytic Efficiency of the Space Shuttle Heat Shield," AIAA Paper 82-0944, June 1982.

[5]Scott, C.D. and Derry, S.M., "Catalytic Recombination and the Space Shuttle Heating," AIAA Paper 82-0841, June 1982.

[6]Kim, M.D., Swaminathan, S., and Lewis, C.H., "Three-Dimensional Nonequilibrium Viscous Shock-Layer Flow Over the Space Shuttle Orbiter," *Journal of Spacecrft and Rockets,* Vol. 21 Jan.-Feb. 1984, pp. 29-35.

[7]Vachris, A.F. and Yaeger, L.S., "QUICK-GEOMETRY: A Rapid Response Method for Mathematically Modeling Configuration Geometry," NASA SP-390, 1975, pp. 49-73.

[8]Helliwell, W.S., Dickinson, R.P., and Lubard, S.C., "Viscous Flow over Arbitrary Geometries at High Angle of Attack," AIAA Paper 80-0064, Jan. 1980.

[9]Bird, R.B., Stewart, W.E., and Lightfoot, E.N., *Transport Phenomena,* John Wiley and Sons, N.Y., 1960.

[10]Szema, K.Y. and Lewis, C.H., "Three-Dimensional Viscous Shock-Layer Flows Over Lifting Bodies at High Angles of Attack," AIAA Paper 81-1146, June 1981.

[11]Hendricks, W.L., "Slip Conditions with Wall Catalysis and Radiation for Multicomponent Nonequilibrium Gas Flow," NASA TM X-64942, June 1974.

[12]Davis, R.T., "Hypersonic Flow of a Chemically Reacting Binary Mixture Past a Blunt Body," AIAA Paper 70-805, July 1970.

[13]Murray, A.L. and Lewis, C.H., "Hypersonic Three-Dimensional Viscous Shock-Layer Flow over Blunt Bodies," *AIAA Journal,* Vol. 16, Dec. 1978, pp. 1279-1286.

[14]Armaly, B.F. and Sutton, K., "Viscosity of Multicomponent Partially Ionized Gas Mixtrues Associated with Jovian Entry," *Aerothermodynamics and Planetary Entry, Progress in Astronautics and Aeronautics,* Vol. 77, edited by A.L. Crosbie, AIAA, N.Y., 1981, pp. 335-350.

[15]Armaly, B.F. and Sutton, K., "Thermal Conductivity of Partially Ionized Gas Mixtures," *Thermophysics of Atmospheric Entry, Progress in Astronautics and Aeronautics,* Vol. 82, edited by Thomas E. Horton, AIAA, N.Y. 1982, pp. 53-67.

[16]Blottner, F.G., Johnson, M., and Ellis, M., "Chemically Reacting Viscous Flow Program for Multi-Component Gas Mixtures," Sandia Laboratories, SC-RR-70-754, Dec. 1971.

[17]Davis, R.T., "Numerical Solution of the Hypersonic Viscous Shock-Layer Equations," *AIAA Journal,* Vol. 8, May 1970, pp. 843-851.

[18]Weilmuenster, K.J. and Hamilton, H.H., II, "A Method for Computation of Inviscid Three-Dimensional Flow Over Blunt Bodies Having Large Embedded Subsonic Regions," AIAA Paper 81-1203, June 1981.

[19]Marconi, F. and Yaeger, L., "Development of a Computer Code for Calculating the Steady Super/Hypersonic Inviscid Flow Around Real Configurations," NASA CR-2675, April 1976.